Optimal market-based operation of microgrid with the integration of wind turbines, energy storage system and demand response resources

Optimal Market-based Operation of Microgrid with the Integration of Wind Turbines, Energy Storage System and Demand Response Resources

Mohammad MansourLakouraj[1], Majid Shahabi[1], Miadreza Shafie-khah[2], João P.S. Catalão[3,*]

[1] *Faculty of Electrical and Computer Engineering, Babol Noshirvani University of Technology, Babol, Iran*
[2] *School of Technology and Innovations, University of Vaasa, 65200 Vaasa, Finland*
[3] *Faculty of Engineering of University of Porto and INESC TEC, 4200-465 Porto, Portugal*

Abstract: This paper deals with an optimal operation of a microgrid in the electricity market and presents the communication between the distribution market operator and microgrid operator. The distribution market operator controls and manages the electricity market established in the distribution level, determining the amount of both electricity price and power exchange between market participants. The microgrid operator is able to purchase active and reactive power from the local distribution market. An effective short-term scheduling of the microgrid is implemented to ensure optimal operation. A risk-based stochastic model is used to model the prevailing uncertainties such as loads, wind generation, and main-grid availability in a market-based operation framework. Moreover, in this model, a linearized AC power flow is added to the mathematical formulations to offer a comprehensive solution to the security-constraint operation of the microgrid. The stochastic operation strategy is formulated as a mixed integer linear programming problem. Regarding the uncertainty modelling, the substation equipment failure is modeled with Monte-Carlo algorithm. The effectiveness of the risk-based stochastic method is demonstrated using a microgrid test bed in the presence of demand response resources, dispatchable and wind generation units as well as energy storage system. The results demonstrate demand response program can significantly reduce the operation cost in worst scenarios. Also, it is indicated that the risk-averse decisions reduce the risk of experiencing costly scenario. The proposed framework incorporating the distribution market constraints reduces the uncertainty in real-time operation as it can specified the required energy before running the problem. The deviations from assigned energy to the microgrid are penalized through the distribution market operator.

Keywords: Microgrid; Wind Generation; Demand Response, Energy Storage System, Distribution Market.

Nomenclature

Sets and Indexes

t	Index of the time periods (1 … T)
ω	Index of each scenario (1 … Ω)
n, m	Index of buses (1 … N)
j	Index of dispatchable DG (1 … J)
l	Index of microgrid lines (1 … L)
b	Index of responsive industrial loads (1 … B)
ξ	Index of responsive industrial load steps
e	Index of ESS (1 … E)
wp	Index of wind turbines (1 … WP)
ca	Index of capacitors (1…CA)

Parameters

$P^{RT}_{\max}, P^{RT}_{\min}$	Maximum/minimum real-time active power transfer of main grid

$Q_{\max}^{RT}, Q_{\min}^{RT}$ Maximum/minimum real-time reactive power transfer of main grid

$S_{n.m}^{feeder}$ Apparent power capacity of line nm

$Q_{n,ca}^{shunt}$ Reactive generated power of capacitor *ca*, at bus *n*

UR_j, DR_j Ramp up/down rate of DG *j*

UT_j, DT_j Minimum up/down time of DG *j*

MC_e, MD_e Minimum charging/discharging hours of ESS *e*

l_{ξ}^{b} Accepted amount of industrial demand reduction

$A_{n,l}$ Element of bus-line matrix (1 if bus *n* is the sending bus of line, -1 if receiving bus, 0 otherwise)

$A_{n,l}^{'}$ Element of modified bus-line matrix (1 if bus *n* is the sending bus of line and 0 otherwise)

b_l, g_l Imaginary/ real parts of admittance of line *l*

x_l, r_l Imaginary/ real parts of impedance of line *l*

ρ_t^M Locational marginal price at common coupling point of microgrid

$IC_{n,t,\omega}^{b}$ Encouraging cost for involvement of industrial consumer *b* at bus *n*

o_{ξ}^{b} Monetary offered by industrial participant *b* at step ξ

$\Gamma_{t,\omega}$ Incentive financial offer for residential consumer

C Penalty cost of deviation from assigned power

k Proportion of active power price

M Large positive scalar

$VOLL_n$ Value of lost load

η Operation efficiency of ESS

$prob_{\omega}$ Happening probability of scenario ω

Variables

$I_{j,t}$ Commitment modes of generation units (1/0 when committed/otherwise)

v_t ESS charging modes (1 means charging states, 0 otherwise)

u_t ESS discharging modes (1 means discharging states, 0 otherwise)

$um_{t,\omega}$ Network connection to microgrid (1/0 when connected/ disconnected)

$x_{t,\omega}$ Power deviation indicator (0 when deviated, 1 otherwise)

$P_{wp,t,\omega}^{wind}$ Output active power of wind turbine

P_t^M, Q_t^M Main grid active/reactive power transfer determined by DMO

$P_{t,\omega}^{RT}, Q_{t,\omega}^{RT}$ Main grid real-time active/reactive power transfer

$\Delta P_{t,\omega}, \Delta Q_{t,\omega}$ Main grid active/reactive power transfer deviation with respect to the determined profile

$\Delta P_{t,\omega}^{+}, \Delta Q_{t,\omega}$ Positive active/reactive power transfer mismatch of main grid

$\Delta P_{t,\omega}^{-}, \Delta Q_{t,\omega}^{-}$ Negative active/reactive power transfer mismatch of main grid

$p_{l,t,\omega}^{loss}, q_{l,t,\omega}^{loss}$ Active /reactive loss of line *l*

$p_{l,t,\omega}^{s}, q_{l,t,\omega}^{s}$ Sending active/reactive power of line *l*

$p_{l,t,\omega}^{r}, q_{l,t,\omega}^{r}$ Receiving active/reactive power of line *l*

$p_{t,\omega}^{n.m}$, $q_{t,\omega}^{n.m}$	Active/reactive power flow between nodes *n* and *m*
$P_{j,t,\omega}^{DG}$, $Q_{j,t,\omega}^{DG}$	Generated active/reactive power of DG *j*
$P_{n,t,\omega}^{Load}$, $Q_{n,t,\omega}^{Load}$	Active/reactive demand at bus *n*
$P_{n,t,\omega}^{C}$, $Q_{n,t,\omega}^{C}$	Active/reactive curtailed consumption atbus *n*
$IP_{n,t,\omega}^{b}$, $IQ_{n,t,\omega}^{b}$	Reduced active/reactive industrial demand *b* at bus *n*
$RP_{n,t,\omega}$, $RQ_{n,t,\omega}$	Diminished active/reactive residential demand at bus *n*
$T_{e,t}^{ch}$, $T_{e,t}^{dch}$	Successive number of charging/discharging hours for ESS *e*
$T_{j,t}^{on}$, $T_{j,t}^{off}$	Successive Number of on/off hours for unit *j*
$\phi_{n,t,\omega}$, $V_{n,t,\omega}$	Angle/ RMS voltage magnitudes of bus *n*
β, α	Risk parameter and confidence level

1. Introduction

Nowadays, microgrids are known as an essential part of the modern power system. These energy systems are autonomous systems comprised of flexible and fixed loads, energy storage systems (ESS) and distributed energy resources (DERs), which can operate in normal and contingency states [1]. The most outstanding feature of microgrids is the islanded operation capability in an emergency situation [2]. Transition to this mode of operation can be initiated by various events such as weather-related incidents, failure of main grid equipment, and intentional disconnection of main grid for upgrading upstream equipment. In addition, islanding happens in response to various disturbances in the main power grid to protect the local resources and reduces the possibility of an interruption in the supply of loads [3].

1.1 Literature review

In recent years, the installation of microgrids in the electric power network has been increased significantly, and scientists anticipate the deployment of microgrid distributes remarkably in the world [4]. The microgrid control strategy is an important issue when microgrids are deployed in power systems. There are three hierarchical control levels, containing primary, secondary and tertiary [5]. The primary and secondary levels address to droop control and voltage/frequency restoration and adjustment while a contingency like sudden changes of loads or power generation as well as islanding transition occurs in the grid. However, the third level allows the operator to schedule microgrid resources in order to attain an economic dispatch (ED) during the interaction with the main-grid [6]. Decision-making problem of microgrid is utilized to minimize operation costs of DERs and power exchange with the upstream network, to provide electrical energy for consumers in a short time period. Two designs are introduced for microgrid control architecture: decentralized and centralized. Decentralized control enables each component to act as an agent having communication with other agents [7]. In contrast, in centralized architecture, a central computing unit is implemented for scheduling and has access to the load and power generation data [8]. This paper focuses on centralized control for microgrid day-ahead

scheduling because this framework is more practical, and does not need financial investments to construct the communication infrastructures. Moreover, it can facilitate the optimization procedure to attain accurate results.

In recent studies, plenty of methods have been suggested to solve short-term planning problem, including stochastic and robust optimization. The robust information decision theory-based scheduling is developed in [9] to optimally manage the energy hubs. Reference [10] proposes a stochastic optimization for microgrid operation in day-ahead and real-time markets. However, the physical constraints of the grid have not been included in these studies. Authors of [11] implement robust optimization for short-term scheduling of multi-carrier energy microgrids. The decomposition technique is also used to enhance the performance of the scheduling. A two-stage robust optimization of multi-energy microgrid is proposed in [12] to supply thermal and electrical loads, but the network physical characteristics have not been modelled with comprehensive power flow modelling. Exhaustive mathematical formulations with the aim of AC power flow, which reflects more realistic models for microgrid operation are used in [13], but they do not investigate the effects of risk constraints on capturing uncertainties

Microgrids allow effective control and integration of many responsive loads which can intensify the demand-side elasticity. Furthermore, energy storage and dispatchable units provide controllable resources, but a price-based scheme is used for their optimal scheduling. By this framework, the utility submits forecasts of microgrids' load, and once the wholesale market assigns the electricity price, the utility sends the actual price signals to each microgrid. Since the demand of consumers is inversely proportional to price signals, this approach can cause new peaks in the power system. In fact, by the increment in the number of price-responsive demands, this challenge would reinforce significantly [14]. A price-based optimal scheduling is proposed in [15], and although the authors consider AC power flow constraints as well as risk measures, they do not suggest a method to cope with unintentional peaks in foreseeable future of smart-grids.

The aforementioned downsides, combined with increasing penetration of microgrids in distribution systems in near-future, have made the case for practicing new methodologies for microgrid operation. Reference [16] proposes stochastic market-based scheduling of microgrid to cope with the mentioned challenges, but physical interpretation of grid and risk constraints have not considered. A comparison makes between market-based and price-based scheduling of microgrid in [17]. The main focus of that is on scheduling from distribution market operator (DMO) perspective without investigating the role of demand response (DR) resources and renewable energy resources (RES) in scheduling process. Reference [18] proposes a market-based optimal scheduling of dependent microgrid considering DR and ESS. The DMO constraints are considered in this study, but the main grid failures are not simulated with time to repair and failure information. Also, the reactive power market is not included in this framework.

DMO is an autonomous entity which is located in distribution grid to monitor and operate the interactions between the independent system operator (ISO) and microgrid operator in the electricity market environment. An efficient designing of electricity market is vital for the future power systems. Reference [19] has delved into the market clearing framework in the presence of microgrids.

1.2 Aims and contributions

Considering existing research works, it can be realized that a few models have been carried out for the optimal operation of microgrid in distribution market environment. Moreover, careful review of the studies discloses that an efficient strategy has not been proposed for addressing uncertainties. Some studies have used varied uncertainties in the scheduling programs as worst-case scenarios [11]. Even though this method simplifies the data preparation and optimization procedure, it does not ensure a realistic approach to the problem, and it would result in an expensive and conservative decision making for scheduling.

In this paper, market-based operation is analyzed from microgrid operator's point of view in the presence of various flexible resources, which is so crucial for future of the electricity market. This study considers the reactive power market beside active power market to ensure a flexible operation of microgrids. This paper also presents a risk-constrained method considering conditional value at risk (CVaR) to make an economic tradeoff between conservative and realistic operations, and to manage different uncertainties such as load behavior, wind, and main-grid outages. The outages of main grid equipment are simulated based on the repair time data. In Table 1, the most relevant research studies to current work are summarized. For each reference, it is shown that whether the items written in the first column of the table were considered or not.

Table 1 Differences of the most relevant works with the current study

References	[10]	[13]	[15]	[16]	[18]	Current study
Equipment failure simulation for main grid	×	×	×	×	×	✓
Risk constraints	×	×	✓	×	✓	✓
AC power flow	×	✓	✓	×	✓	✓
Market-based operation	×	×	×	✓	✓	✓
Reactive power market	×	×	×	×	×	✓

There are a few research works that have optimized the operation cost of microgrid in the presence of AC power flow equations, distribution market operator (DMO) constraints, DR resources, ESS, and risk constraints as well as considering islanded mode of operation. On these bases, the new contributions of this paper can be listed as follows:

- Developing a stochastic scheduling model for market-based operation based on DMO constraints and risk formulations;
- Considering the positive operational role of DMO in modern reactive and active power markets;
- Employing the linearization procedure of nonlinear AC power flow formulations to guarantee the operational security;
- Considering uncertainties associated with load and RESs as well as simulating main-grid connection failure with time to failure and repair ;
- Investigating the role of ESS and DR resources as well as risk and financial penalty on daily operation.

The remainder of this paper is arranged as follows. Section 2 deals with the theoretical bases of the scheduling scheme. In Section 3, mathematical formulations are proposed. Numerical assessments and results are given in Section 5. As a final part, Section 6 and 7 presents notable discussion and conclusions of this study, respectively.

2. Theoretical basis of the proposed method

The proposed method is a short term market-based scheduling of the resources in a microgrid. The detailed components of this energy system are characterized as follows:

2.1. Distribution market operator

DMO, cooperating with ISO in the electricity market, is proposed to provide a competitive environment in distribution system for exchanging electrical power between grid participants. DMO allows network operation and electricity market activities, coordinates with the utilities to develop the planning investment. This operator also ensures active communication with the ISO to negotiate power purchases and awarded bids for attaining reliable operation in power system. Moreover, DMO facilitates the intense penetration of microgrids from system operator's point of view, and it addresses prevailing integration hurdles. For the sake of addressing the deficiencies of price-based operation, a market-based method is suggested where the DMO determines the demand of microgrid and this package of demand is known as a certain value in the scheduling horizon. This mediator player will contribute to reduce peak loads in the systems, so the reliability and efficiency of the operation would satisfy. In fact, DMO acts as a player between the ISO and microgrids that helps microgrid to participate in reactive and active power markets and coordinates the upstream grid with microgrids to minimize the risk of uncertainties [14]. Then, several demand bids are collected by DMO from different microgrids, and they are combined to propose an aggregated bid to the ISO. Combined active and reactive demand bids and generation bids of generation companies are received to specify the electricity price. In addition, after performing market clearing procedure and determining schedule of each connected participant, microgrids shares are determined by DMO from the awarded electrical energy [16]. Since the amount of power transfer to the microgrids is announced to the microgrid operator, it eliminates a significant part of uncertainties caused by price-responsiveness of operator [17]. It is to be noted that this research concentrates on modeling the day-ahead scheduling of microgrid under distribution market environment from operator's perspective. Therefore, implementation of DMO can remarkably fix different challenges such as uncertainties and sharp peaks that microgrid operator and utilities face during the scheduling process. Figure 1 clearly demonstrates the interaction of DMO with ISO and microgrid.

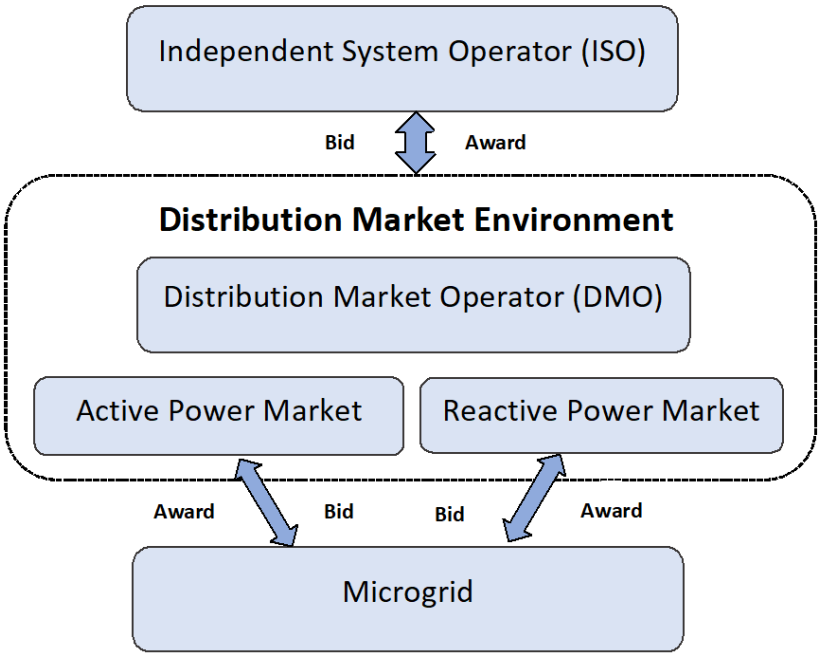

Fig. 1. Proposed microgrid electricity market participation by DMO

2.2. Uncertainties

In this scheduling process, microgrid operator faces uncertainties of wind generation, loads and electrical network unavailability. In this section different approaches for simulating uncertainties will discuss in detail:

In a power system comprising feeders, substations, and DERs, the outages of equipment are probable, so the availability of such components can be contemplated as an uncertain variable. Considering these inevitable failures, microgrid operator should implement a practical approach to model these incidents. In this paper, the probable outages of the substation which microgrid procure power from are considered. The availability of this substation is explained by time to failure (t_F), and time to repair (t_R) parameters, which both constitute random variables in the functions according to (1a)–(1b).

$$t_F = -MTTF \times \ln(u_F) \tag{1a}$$

$$t_R = -MTTR \times \ln(u_R) \tag{1b}$$

MTTF and MTTR are defined as mean time to failure and mean time to repair, respectively. Furthermore, u_F and u_R are random variables which are distributed between 0 and 1 uniformly. The availability scenario generation algorithm is discussed profoundly in [20], which is used in main-grid availability simulations.

Based on historical data, wind generation scenarios are generated using the autoregressive moving-average (ARMA). According to ARMA (x,y) model, the future values of a numerical pattern has a linear mathematical function of past values, and the amounts of noise as (2).

$$z_t = \varepsilon_t - \sum_{j=1}^{y} \Theta_j \varepsilon_{t-j} + \sum_{j=1}^{x} \Phi_j z_{t-j} \tag{2}$$

In this formulation, Ɛ, y, and x stand for the uncorrelated stochastic procedure, moving average parameters θ_1, θ_2 …θ_y, autoregressive parameters ϕ_1, ϕ_2…ϕ_x , respectively. Moreover, the uncorrelated stochastic process refers to white noise through zero mean and σ_ε^2 variance [10].

The load's behavior depends on the weather condition during a day and social events. It is evident that the consumption patterns of people on the weekends are not similar to regular days. The Gaussian probability distribution function proposed in (3) is a reliable choice to simulate uncertain parameters of loads [15]. Both σ and μ are the standard and average deviation of historical records for corresponding demands (l) [21].

$$f_d(l) = \left(\frac{1}{\sigma\sqrt{2\pi}}\right) \times \exp\left(-\frac{(l-\mu)^2}{2\sigma^2}\right) \quad (3)$$

Using the aforementioned methods for generating different scenarios, a vector of scenarios for all hours is provided with the same probability. It is vital to determine a reasonable number of scenarios to satisfy accuracy concerns and to reduce computational times for this simulation. The number of scenarios is reduced using the forward approach in SCENRED tool in GAMS [22]. As a result, these reduced scenarios are a compromise between the complexity of the problem and the precision of the final results. Figure 2 demonstrates the flowchart of scenario generation process for different uncertainties.

2.3. Proposed method

Microgrid operator needs to consider microgrid economy and find the least-cost decisions in scheduling. This issue is taken in to account in this study while considering several uncertainties associated with wind generation, load forecast, and main-grid outages. A massive number of scenarios accompanied with uncertain parameters is generated and then reduced through reduction methods to guarantee feasible and efficient mode. In this study, risk constraints are added to the stochastic framework, and these constraints manage the costly scenarios caused by incidents like equipment failure in main-grid. A 24-h scheduling horizon is assumed, so DGs and ESS are committed hourly. After the microgrid operator sends its required electrical energy signal (demand) to the DMO one day ahead, the DMO will determine the price of active and reactive power markets and the amount of accepted demand for all operation period of time. Therefore, according to the determined day-ahead demand profile, the microgrid operator will solve the scheduling problem with fewer uncertain parameters. It is also assumed that deviations from the determined power by the DMO will be penalized based on pre-determined value. This penalty is just imposed to the operator whenever the deviation is positive, i.e., the real-time electrical energy transfer is greater than the determined energy profile. Figure 3 demonstrates the whole market-based scheduling process of microgrid. The first stage decisions are related to the commitments of conventional DGs and setting ESS charging/discharging hours. Decisions at the second stage are associated with deviation of power transfer from DMO's determined program, calculating the financial penalty of operation, economic dispatch of ESS and DGs, DR resources elasticity and load curtailments as well as optimal power flow of microgrids' lines. In the following, the mathematical interpretation of objective function and constraints are presented.

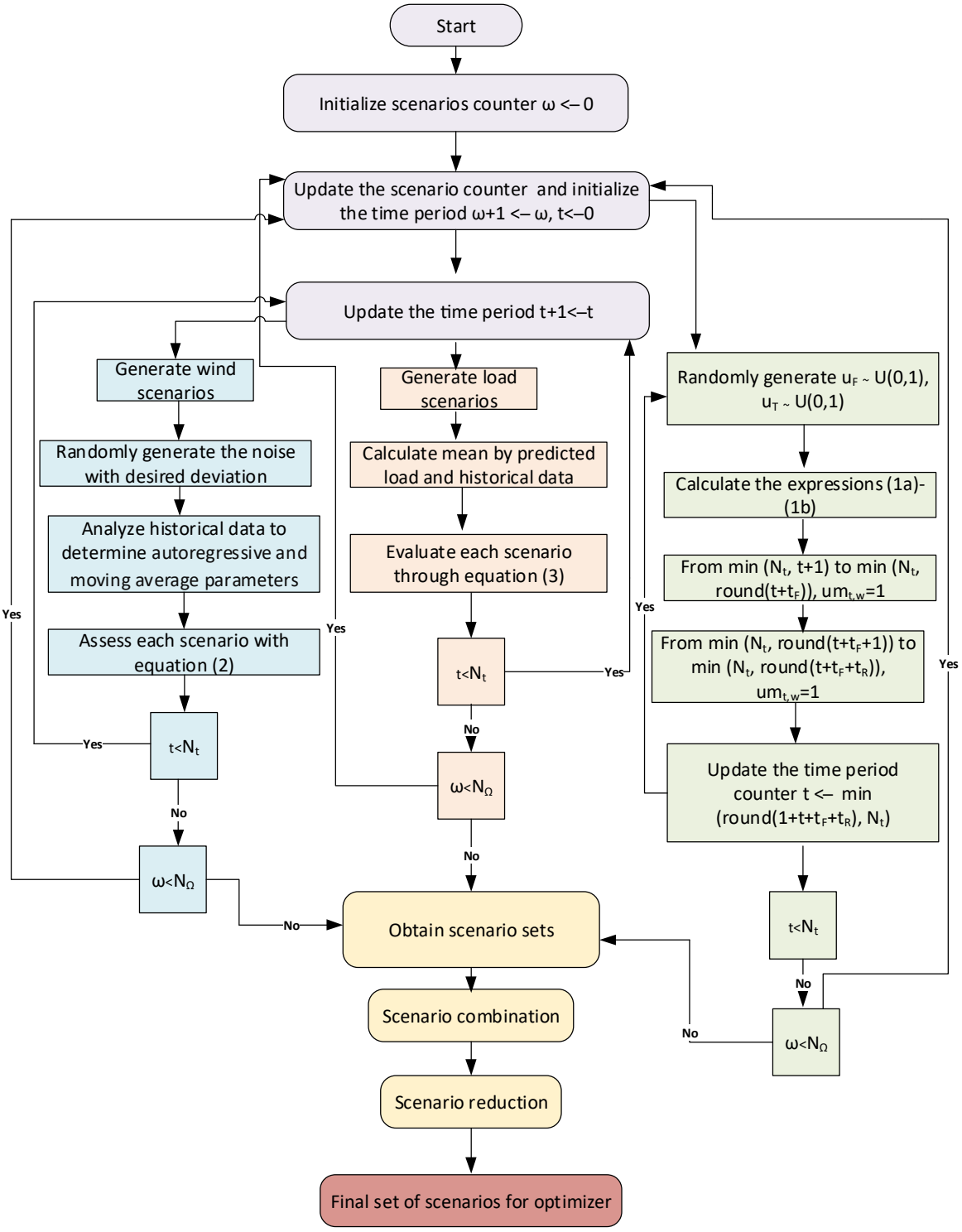

Fig. 2. Flowchart of scenario generation

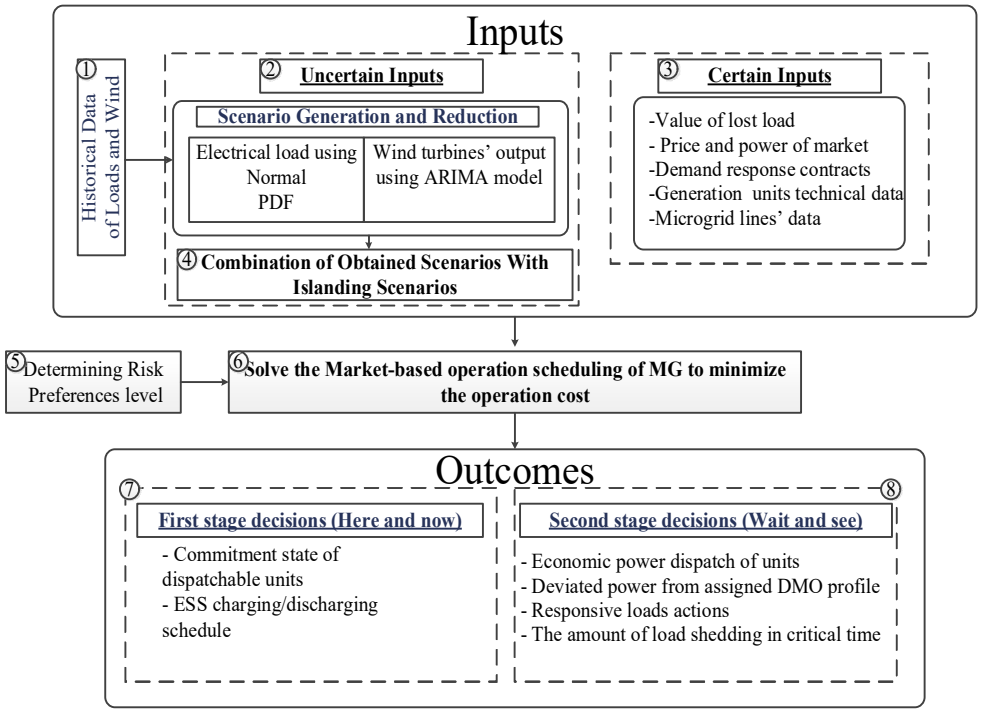

Fig. 3. Presented framework for microgrid operation

3. Problem formulation

The market-based operation scheduling problem of microgrid is formulated as a mixed-integer linear programming (MILP). The objective of this problem and its constraints are described as follows.

3.1. Objective function

The objective function in (4a)–(4b) is to minimize the operation cost over scheduling horizon in the microgrid, including the cost of buying active and reactive power from the electricity market, the penalty for deviation from determined active and reactive power transfer from upstream, operation costs of dispatchable DGs, load curtailment costs and DR resources participation value. It is to be noted that the first two terms related to the main-grid power transactions have fixed amount because they are scheduled by DMO before 24-h scheduling horizon. Moreover, there is no market-clearing method for reactive power in electricity market, so in this study, the reactive power price is supposed to be 0.1 of locational marginal price (i.e. k=0.1) in PCC bus [23].

$$OF = Min\sum_{t=1}^{T}\{\rho_t^M P_t^M + k\rho_t^M Q_t^M + \sum_{\omega=1}^{\Omega} prob_\omega \, \mathrm{C}(\omega)\} \tag{4a}$$

$$\mathrm{C}(\omega) = c\Delta P_{t,\omega}^{+} + kc\Delta Q_{t,\omega}^{+} + \sum_{j\in J} F(P_{j,t,\omega}^{DG}) + \sum_{n\in N} P_{n,t,\omega}^{LC} VOLL_n + \sum_{b\in B} IC_{n,t,\omega}^{b} + \sum_{n\in N} RP_{n,t,\omega}\Gamma_{t,\omega} \tag{4b}$$

3.2 Constraints

The set of technical and economic constraints of scheduling process are as follow:

1) Distribution market constraints

The DMO schedules and determines the upstream grid electrical power transfer for microgrid. However, the microgrid operator is able to violate the assigned power profile and pay financial penalty as presented in (5a)–(5j).

$$P_{\min}^{RT} um_{t,\omega} \le P_{t,\omega}^{RT} \le P_{\max}^{RT} um_{t,\omega} \tag{5a}$$

$$Q_{\min}^{RT} um_{t,\omega} \le Q_{t,\omega}^{RT} \le Q_{\max}^{RT} um_{t,\omega} \tag{5b}$$

$$\Delta P_{t,\omega} = P_{t,\omega}^{RT} - P_t^M \tag{5c}$$

$$\Delta Q_{t,\omega} = Q_{t,\omega}^{RT} - Q_t^M \tag{5d}$$

$$\Delta P_{t,\omega} = \Delta P_{t,\omega}^{+} - \Delta P_{t,\omega}^{-} \tag{5e}$$

$$\Delta Q_{t,\omega} = \Delta Q_{t,\omega}^{+} - \Delta Q_{t,\omega}^{-} \tag{5f}$$

$$0 \le \Delta P_{t,\omega}^{+} \le M(1 - x_{t,\omega}) \tag{5g}$$

$$0 \le \Delta P_{t,\omega}^{-} \le M x_{t,\omega} \tag{5h}$$

$$0 \le \Delta Q_{t,\omega}^{+} \le M(1 - x_{t,\omega}) \tag{5i}$$

$$0 \le \Delta Q_{t,\omega}^{-} \le M x_{t,\omega} \tag{5j}$$

Constraints (5a)–(5b) demonstrates the active and reactive power transfer from the utility level. The binary variable $um_{t,\omega}$ is generated in each scenario to simulated islanding occurrence by zeroing out the distribution market power transfer. The upstream grid active and reactive power transfer violation from the imposed power profile of DMO is set by (5c) and (5d), respectively. If the mismatch of active and reactive power transfer of the upstream grid is positive, the cost function is penalized, where $x_{t,\omega}$=0 and $\Delta P^{+} = \Delta P$, $\Delta Q^{+} = \Delta Q$ exercising (5e)–(5j). M is a large positive scalar which determines the maximum deviation of real-time power transfer [16].

2) Power balance equations

Equations (6a) and (6b) guarantee the active and reactive electrical power balances at the point of common coupling (PCC) in which microgrid links to the upstream network. For the other buses of microgrid, the electric generation and consumption balances are the same as (6c) and (6d). The generation of ESS, DG and wind turbines as well as DR resources are added to these equations.

$$P_{t,\omega}^{RT} - \sum_{l \in L} A_{n,l} p_{l,t,\omega}^{s} - \sum_{l \in L} A_{n,l}^{'} p_{l,t,\omega}^{loss} = 0 \; ; \; n = 1 \tag{6a}$$

$$Q_{t,\omega}^{RT} - \sum_{l \in L} A_{n,l} q_{l,t,\omega}^{s} - \sum_{l \in L} A_{n,l}^{'} q_{l,t,\omega}^{loss} = 0 \; ; \; n = 1 \tag{6b}$$

$$\sum_{j \in J_n} P_{n,j,t,\omega}^{DG} + \sum_{e \in E_n} P_{n,e,t,\omega}^{ESS} + \sum_{wp \in WP_n} P_{n,wp,t,\omega}^{wind} - \sum_{l \in L} A_{n,l} p_{l,t,\omega}^{s} - \sum_{l \in L} A_{n,l}^{'} p_{l,t,\omega}^{loss} - P_{n,t,\omega}^{Load} + IP_{n,t,\omega}^{b} + RP_{n,t,\omega} + P_{n,t,\omega}^{LC} = 0 \; ; \; \forall n \ne 1 \tag{6c}$$

$$\sum_{j\in J_n} Q^{DG}_{n,j,t,\omega} + \sum_{ca\in CA_n} Q^{Shunt}_{n,ca} - \sum_{l\in L} A_{n,l} q^{s}_{l,t,\omega} - \sum_{l\in L} A^{'}_{n,l} q^{loss}_{l,t,\omega} - Q^{Load}_{n,t,\omega} + IQ^{b}_{n,t,\omega} + RQ_{n,t,\omega} + Q^{LC}_{n,t,\omega} = 0 \; ; \forall\, n \neq 1 \tag{6d}$$

3) Linearized power flow equations

In this section, the linear power flow equations are represented based on the method explained in [24]. The equations of active/reactive power flows at sending and receiving points of the line *l*, connecting bus n to bus m, are expressed as (7a)–(7d). The power loss expression is non-linear, and it is converted to linear terms using piecewise linearization technique [15].

$$p^{s}_{l,t,\omega} = g_l (V_{n,t,\omega} - V_{m,t,\omega}) + \frac{1}{2} p^{loss}_{l,t,\omega} - b_l \phi_{n,t,\omega} + b_l \phi_{m,t,\omega} \tag{7a}$$

$$p^{r}_{l,t,\omega} = -g_l (V_{m,t,\omega} + V_{n,t,\omega}) + \frac{1}{2} p^{loss}_{l,t,\omega} - b_l \phi_{m,t,\omega} + b_l \phi_{n,t,\omega} \tag{7b}$$

$$q^{s}_{l,t,\omega} = b_l (-V_{n,t,\omega} + V_{m,t,\omega}) + \frac{1}{2} q^{loss}_{l,t,\omega} - g_l \phi_{n,t,\omega} + b_l \phi_{m,t,\omega} \tag{7c}$$

$$q^{r}_{l,t,\omega} = b_l (V_{m,t,\omega} - V_{n,t,\omega}) - \frac{1}{2} q^{loss}_{l,t,\omega} + g_l \phi_{m,t,\omega} + g_l \phi_{n,t,\omega} \tag{7d}$$

4) Conventional DGs constraints

The constraints of conventional generation unit are listed as (8a)–(8f). The production of these dispatchable units obeys constraints (8a)–(8b). The binary variable $I_{j,t}$ demonstrates the commitment status of each unit. The unit's ramp up/down rate restrictions are shown by (8c)–(8d), satisfying the fast or slow changes in generation output. The minimum up/down hour limits are subjected to (8e)–(8f) [15], indicating the time period of the operation.

$$P^{DG,\min}_{j} I_{j,t} \le P^{DG}_{j,t,\omega} \le P^{DG,\max}_{j} I_{j,t} \tag{8a}$$

$$Q^{DG,\min}_{j} I_{j,t} \le Q^{DG}_{j,t,\omega} \le Q^{DG,\max}_{j} I_{j,t} \tag{8b}$$

$$P^{DG}_{j,t,\omega} - P^{DG}_{j,t-1,\omega} \le UR_j \tag{8c}$$

$$P^{DG}_{j,t-1,\omega} - P^{DG}_{j,t,\omega} \le DR_j \tag{8d}$$

$$UT_j (I_{j,t} - I_{j,t-1}) \le T^{on}_{j,t} \tag{8e}$$

$$DT_j (I_{j,t-1} - I_{j,t}) \le T^{off}_{j,t} \tag{8f}$$

5) Energy storage system constraints

Technical constraints of ESS are presented in this section. The power level of ESS is obtained by (9a). Charging and discharging process at time slots are confined through (9b)–(9c). The charging and discharging of this system should not happen simultaneously as enforced by (9d). The state of charge (SOC) in ESS and its limitation is proposed in (9e)–(9f). The SOC is a function of its value in previous time slot and ESS power. The minimum time period of charging and discharging is satisfied by (9g) and (9i), respectively [10].

$$P^{ESS}_{e,t,\omega} = P^{ESS,dch}_{e,t,\omega} - P^{ESS,ch}_{e,t,\omega} \tag{9a}$$

$$P_e^{dch,\min} u_t \le P_{e,t,\omega}^{ESS,dch} \le P_e^{dch,\max} u_t \quad (9b)$$

$$P_e^{ch,\min} v_t \le P_{e,t,\omega}^{ESS,ch} \le P_e^{ch,\max} v_t \quad (9c)$$

$$u_t + v_t \le 1 \quad (9d)$$

$$SOC_{e,t,\omega} = SOC_{e,t-1,\omega} - (1/\eta) P_{e,t,\omega}^{ESS,dch} + \eta P_{e,t,\omega}^{ESS,ch} \quad (9e)$$

$$SOC_e^{\min} \le SOC_{e,t,\omega} \le SOC_e^{\max} \quad (9f)$$

$$MC_e \left(u_t - u_{t-1}\right) \le T_{e,t}^{ch} \quad (9g)$$

$$MD_e \left(v_t - v_{t-1}\right) \le T_{e,t}^{dch} \quad (9i)$$

6) Bus voltage bounds

In (10), bus voltage is confined within its acceptable bound, which is between 0.95 p.u and 1.05 p.u. PCC bus is considered as the reference point of system, and its voltage is regulated by the main grid.

$$0.95 \le V_{n,t,\omega} \le 1.05 \quad (10)$$

7) Load curtailment limits

The determined amount of curtailed load should be less than the base demand in buses according to the constraints (11a)–(11b). Furthermore, constant power factor is ensured by (11c) after load shedding. These load curtailment representations are also known as unintentional load shedding constraints.

$$0 \le P_{n,t,\omega}^{C} \le P_{n,t,\omega}^{C,\max} \quad (11a)$$

$$0 \le Q_{n,t,\omega}^{C} \le Q_{n,t,\omega}^{C,\max} \quad (11b)$$

$$P_{n,t,\omega}^{C} Q_{n,t,\omega}^{L} = Q_{n,t,\omega}^{C} P_{n,t,\omega}^{L} \quad (11c)$$

8) Demand response constraints

In the Interruptible/Curtailable (I/C) program, the system operator sends incentive price signals to electricity consumers [25]. After receiving these signals by responsive loads, they decide whether to participate in this program or not. Industrial consumers have price steps, and each step has a specific price due to the contract. The DR participation constraints are presented as (12a)–(12d) [26]. L_{ξ}^{b} and L_{min}^{b} are the maximum and minimum demand reductions in steps ξ and one, respectively. Also, at each time slot, the summation of reduced consumption cannot be greater than L_{ξ}^{b}. Moreover, a predefined portion of the aggregated residential demand is diminished, and the related constraints of residential DR program are presented as (13a)–(13b) [18].

$$L_{\min}^{b} \le l_1^{b} \le L_1^{b} \quad (12a)$$

$$0 \le l_{\xi}^{b} \le (L_{\xi+1}^{b} - L_{\xi}^{b}); \forall \xi = 2,3... \quad (12b)$$

$$IP_{n,t,\omega}^{b} = \sum_{\xi=1} l_{\xi}^{b} \quad (12c)$$

$$IC_{n,t,\omega}^{b} = \sum_{\xi=1} o_{\xi}^{b} l_{\xi}^{b} \quad (12d)$$

$$0 \le RP_{n,t,\omega} \le RP_{n,t,\omega}^{\max} \quad (13a)$$

$$0 \le RQ_{n,t,\omega} \le RQ_{n,t,\omega}^{\max} \quad (13b)$$

9) *Risk constraints*

Risk expression is commonly used in the objective functions [27], but they can be included as constraints in the formulations of economic problems [28]. In this study, constraints (14a)–(14d) are utilized to capture the effects of the uncertainties in the scheduling period. From the mathematical perspective, CVaR is defined as (14a), and the VaR is a measure that refers to the minimum value of a number of costs. Constraint (14b) imposes the risk preferences level within a determined β as a risk parameter which defines the compromise between the expected value of objective function and risk aversion. In fact, the amount of this parameter is subject to the operator's preference about risk-constrained controlling strategy. A risk-taker decision maker prefers a value larger than one, but a risk-averse person prefers a value close to one during the scheduling process [15]. The amount of this parameter can be easily adjusted according to the probable scenarios.

$$CVaR = \frac{1}{(1-\alpha)} \sum_{\omega=1}^{\Omega} prob_{\omega} \eta_{\omega} + VaR \quad (14a)$$

$$CVaR \le \beta \times OF \quad (14b)$$

$$\sum_{t=1}^{24} \{\rho_t^M P_t^M + k\rho_t^M Q_t^M + c\Delta P_{t,\omega}^{+} + kc\Delta Q_{t,\omega}^{+} + \sum_{g\in G} F(P_{g,t,\omega}^{DG}) + \sum_{n\in N} P_{n,t,\omega}^{LC} VOLL_n + \sum_{b\in B} IC_{n,t,\omega}^{b} + \sum_{n\in N} RC_{n,t,\omega}\Gamma_{t,\omega} - VaR - \eta_{\omega} \le 0\} \quad (14c)$$

$$\eta_{\omega} \ge 0 \quad (14d)$$

4. Test system

The proposed risk-based operation scheduling problem is applied to a typical test system (see Figure 4). The microgrid characteristics such as line data are borrowed from [10]. Specifications of installed generation units are given in Table 2.

Table 2. Characteristics of ESS, conventional DGs, and the total capacity of wind turbines

Dispatchable Units	Connection BUS	Marginal Cost (€/MWh)	Min/Max Generation Power (MW)	Min Up/ Down hours	Ramp Up/Down Limit (MW/h)
U1	5	63	1-4	2	0.5
U2	16	85	0.8-3	1	2
U3	15	90	0.4-2	1	1.6
ESS	3	-	0.4-2	5	-
Wind turbines	10,12,20	-	0-3	-	-

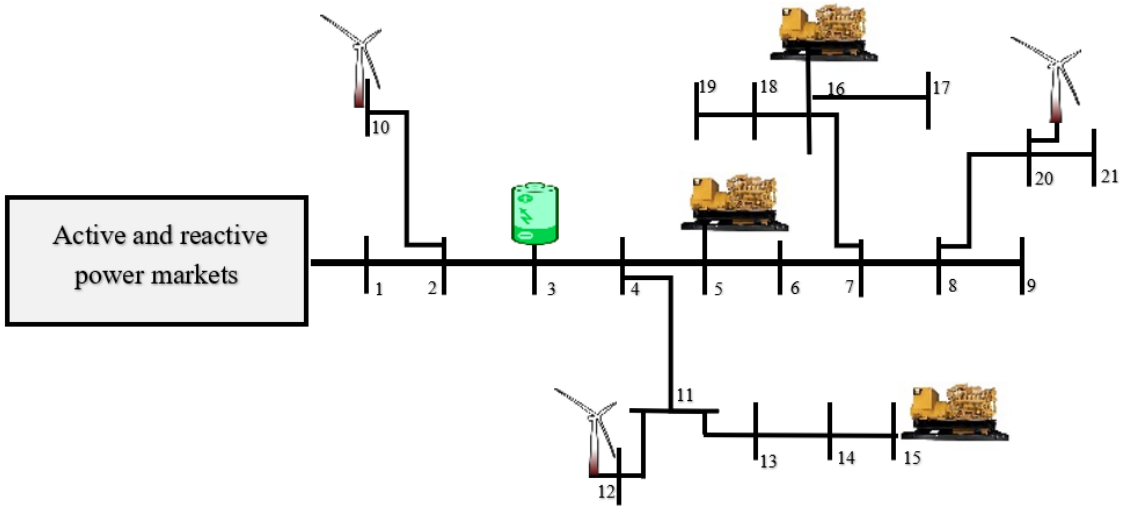

Fig. 4. Single line schematic of microgrid test system

As mentioned about scenario generation and reduction avenues in Section 2.2, seven scenarios, each consisting of a vector of upstream network unavailability states, wind turbines power output and load patterns are calculated through SCENRED.

Three wind turbines with a total power capacity of 3 MW are installed at three buses. The power generation of these turbines is simulated based on historical data derived from national renewable energy laboratory [29]. As microgrid's buses are located in a small urban region, the output power of each wind turbine is similar to other turbines. Figure 5 demonstrates the aggregated wind turbines output in a typical day.

Figure 6 shows the total industrial and residential loads in various scenarios. Industrial demands are considered in buses 10 and 21, but the residential loads are distributed in other buses of the microgrid with 0.95 power factor. The industrial loads have almost certain behavior, but residential loads follow a normal probability distribution function with a standard deviation of 25% and mean value equal to the forecasted loads.

The random parameters associated with the availability of the upstream network is determined by Monte-Carlo algorithm [20]. In this method, MTTF and MTTR can be determined according to the historical data of main-grid outages, which is discussed in [30]. An availability states of the main grid is a chronological set of binary (0, 1) variables. Zero shows the outages of main grid; however, one ensures the grid connected mode of operation. Table 3 illustrates the connection statues of microgrid to the upstream grid in all scenarios. Figure 7 depicts the scheduled upstream power transfer and locational marginal price (LMP) in PCC node, with a violation penalty of €70.5/MWh.

In this microgrid, operator encourages the residential and industrial consumers to take part in the DR program by proposing financial advocates. The DR price-quantity steps for the participation of industrial customers in the DR program is indicated in Table 4. It means that in each step, the power consumption of industrial loads can be reduced up to the maximum power capacity referred in Table 4. Then, the operator should pay the cost of loads' participation in DR program according to price offers shown in the table

for all steps. Moreover, it is supposed that 10% of the residential demands are permitted to be diminished. The financial incentives for these consumers are presented in [10].

In what follows, the market-based scheduling of the microgrid is solved by CPLEX on a computer with 2.2 GHz processor and 8GB RAM considering min gap of 0%, and the numerical studies of microgrid operation are argued precisely.

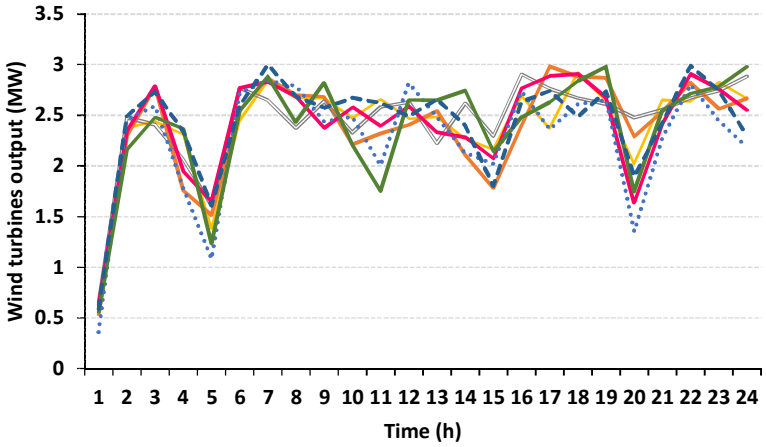

Fig. 5. Output active power of wind turbines

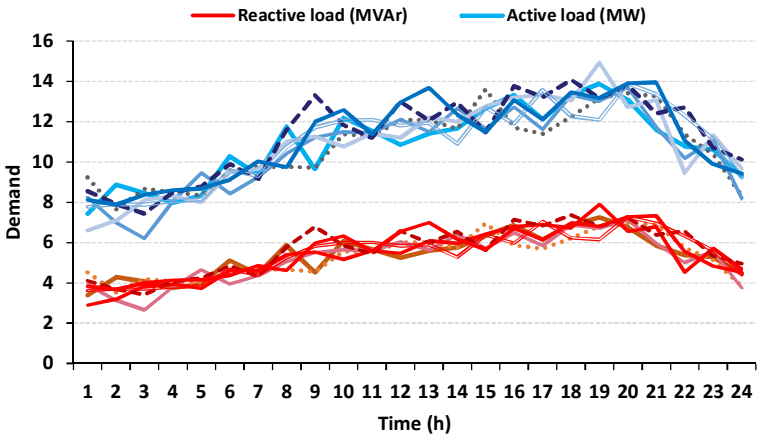

Fig. 6. Demand profile of microgrid

Table 3. Upstream grid connection and disconnection modes in each scenario

Time (h)	Scenario number						
	S1	S2	S3	S4	S5	S6	S7
1	0	1	1	1	1	1	1
2	0	1	1	1	1	1	1
3	0	1	1	1	1	1	1
4	0	1	1	1	1	1	1
5	1	1	1	1	1	1	1
6	1	1	1	0	1	1	1
7	1	1	1	0	1	1	1
8	1	1	1	0	1	1	1
9	1	1	1	0	1	1	1
10	1	1	1	0	1	1	1
11	1	1	1	0	1	1	0
12	1	1	1	1	1	1	0
13	1	1	1	1	0	1	0
14	1	0	1	1	0	1	0
15	1	0	1	1	0	1	0
16	1	0	1	1	0	1	0
17	1	0	1	1	0	1	0
18	1	0	1	1	0	1	1
19	1	1	1	1	0	1	1
20	1	1	1	1	0	1	1
21	1	1	1	1	1	1	1
22	1	1	1	1	1	0	1
23	1	1	1	1	1	0	1
24	1	1	1	1	1	0	1

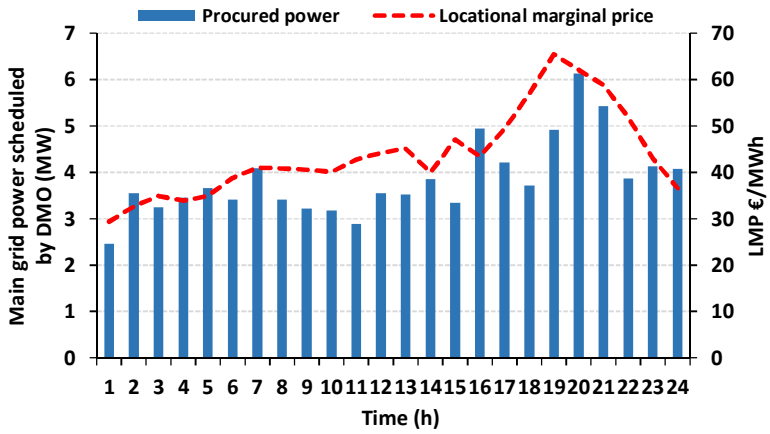

Fig. 7. Scheduled power and price for microgrid by distribution market

5. Numerical analysis

In this problem, the risk parameters α and β are adjusted to be 0.7 and 1.03, respectively. The optimal market-based operation scheduling of microgrid is executed.

Table 4. Industrial DR price and power

	Industrial loads	DR price-quantity steps			
		1	2	3	4
Maximum power capacity (MW)	**A**	0.1	0.2	0.2	0.1
	B	0.2	0.1	0.1	-
Price offers (€/MWh)	**A**	160	230	320	470
	B	185	300	520	-

The calculated expected operation cost and CVaR are €11958 and €12317 in this simulation process, respectively. The VAR amount shows the minimum values of the worst scenarios' cost. More details of related costs can be seen in Table 4. It is to be noted that the expected cost of DR participation is not significant since the occurrence probability of scenarios with the islanded mode of operation is low, and mathematically, DR expected cost cannot explain the details very well. Therefore, it is better to refer to the DR cost and occurrence probability, which are €661.17 and 0.0077 for worst scenario (scenario 5). Furthermore, Figure 8 depicts the participation of flexible load in DR program for each scenario. It can be observed that in scenario 3, DR resources do not participate in DR program because there are sufficient energy resources to supply the loads, but in scenario 5, 6.07MWh energy is diminished to minimize unplanned load shedding. More specifically, Figure 9 demonstrates the load behavior after implementing DR in scenario 5. The demand is reduced in peak hours, which reduces operation cost and guarantees reliability of the network.

The expected penalty cost shows the deviation of power from the scheduled electrical power profile of DMO. In fact, the assigned power is not always enough for microgrid loads' consumption, so the operator decides to procure more electrical energy, and pay the penalty for this deviation.

Figure 10 illustrates the differences between DMO profile and real-time power for grid connected mode of operation (scenario 3). The amount of active power deviation is 5.74 MWh in 24 hours for this scenario.

Table 5 Details of operation costs

Operation cost (€)	11958.2
CVaR (€)	12317
VaR (€)	11803.9
Cost of purchased energy from distribution market (€)	4435.6
Penalty of deviation (€)	416.5
DR participation cost(€)	21.4
Dispatchable DGs production cost (€)	7084.7

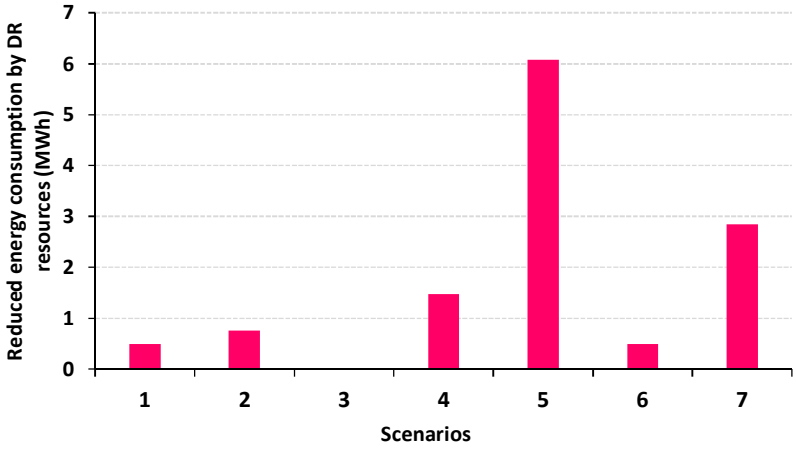

Fig. 8. Reduction of energy demand during a day by DR resources

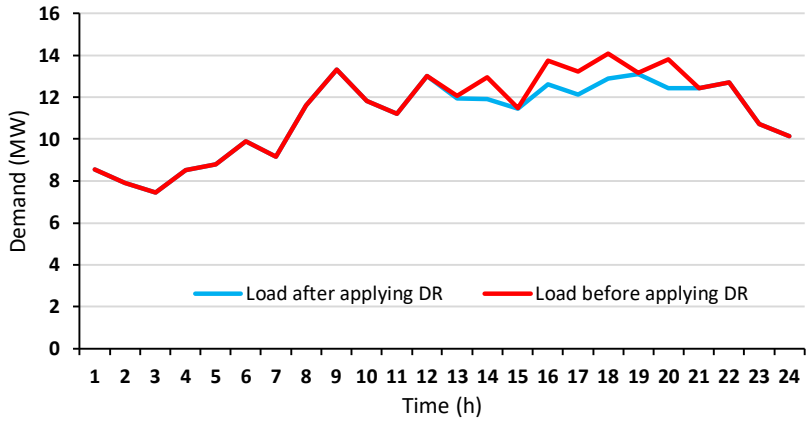

Fig. 9. The demand of customers in scenario 5 with and without DR application

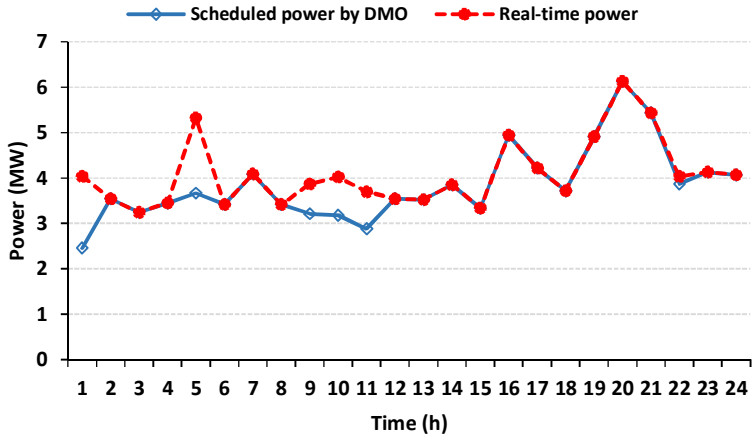

Fig. 10. Differences between scheduled and real-time power in scenario 3

Generation units have remarkable participation in providing electrical energy of consumers. The production cost of dispatchable units is €7084.7, and it means that 59.3% of the power generation cost depends on these resources. The operation costs of ESS and wind turbines are neglected as they have small costs in 24-h horizon. Furthermore, dispatchable DGs participate in islanded hours to compensate for the energy shortages and reduce the unintentional load shedding. Figure 11 demonstrates the procured electrical energy for the worst scenario. As shown in this figure, dispatchable units are fully committed to provide the consumers' energy in islanded hours (i.e. hours 13-20), while in other hours, units 1 and 2 mainly produce electrical energy besides other resources.

The ESS discharging pattern illustrates that 76% of ESS power capacity is allocated to islanded hours in scheduling procedure, and the charging hours are programmed between 2 am and 9 am when energy resources can supply loads without power shortages. It is worth mentioning that power loss of microgrid system is small because there are several flexible resources that can reduce the power congestion of feeders, but during the islanded hours paying attention to power loss is important. Considering Figure 11, it is evident that the loss is increased %38.8 on average during islanding period of time in comparison to grid-connected hours. In fact, increasing the congestion of the feeders due to the high participation of DGs for supplying loads in these hours, and conveying power to different areas of the microgrid intensifies the power loss in the system lines.

In addition, the modified load is the result of DR participation that changes the pattern of the loading in this scenario. It is shown that DR resources reduce their consumption in islanded hours to ensure power production and consumption balance.

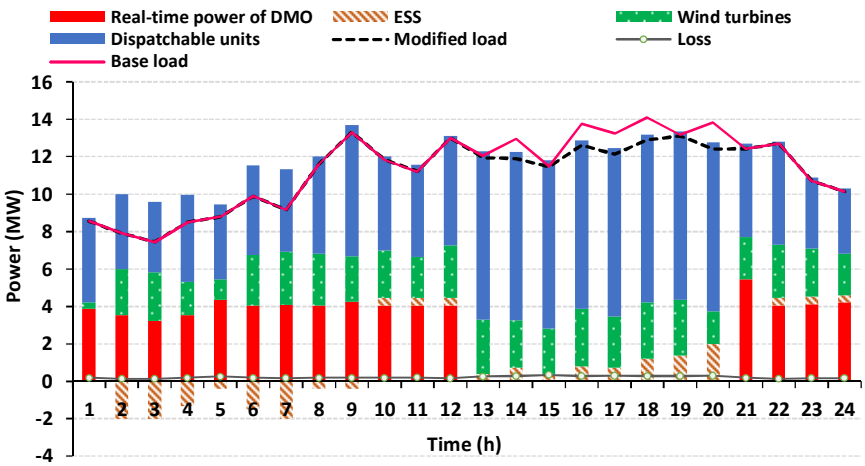

Fig. 11. Optimal scheduling of energy resources

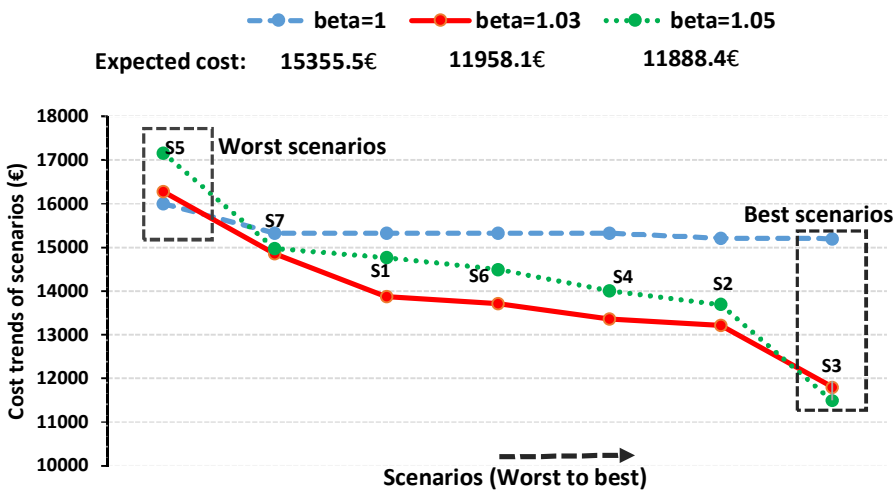

Fig. 12. Scenarios' cost trends in different risk preferences level

5.1. Sensitivity analysis

a) Risk parameter (β)

In this part, the effects of changing β parameter on various scenarios are evaluated. The amount of β is subject to the microgrid operator's preferences for mitigating the risk of uncertainties. A risk-averse operator inclines to choose a value of this parameter close to one in order to confront with imposed risks, while a risk-taker person sets β on a larger value. By risk-taking strategy, the operator will face cheaper expected operation cost, but the operator cannot significantly reduce the operation costs of worst or expensive scenarios. Figure 12 depicts the operation costs in different scenarios and the expected cost of each strategy is shown beside their trends. As shown in the picture, when the β gets closer to 1, the cost of the worst scenarios decreases; however, the cost of cheaper scenarios increases. Therefore, the expected cost in this strategy will attain a higher amount. On the contrary, when the operator chooses a higher amount of β for scheduling, the costs of cheaper scenarios diminishes, but the cost of expensive scenario increases. In this situation, since the number and the occurrence probability of cheaper scenarios are higher, they can reduce the value of expected cost. It might be good news for the operator, but if the worst scenario happens in the day-ahead scheduling, it can impose an expensive cost of operation. As a result, it is better to find a trade-off between the risk-averse and risk-taker strategy by adjusting β. In this study, choosing β=1.03 is an appropriate choice as it reduces costs of 5 scenarios more than two other strategies. Moreover, in comparison to the high risk-taking policy (β =1.05), it also reduces the cost of worst scenario from €17161.28 to €16275.31, which means that suitable adjustment of β provides rational results. The expected cost of this middle strategy is 28.4% lower than risk-averse (β =1) short-term planning. It is to be noted that best scenarios are related to the grid-connected operation with the highest probability of occurrence (i.e. 0.936), so this is why the value of expected costs is close to the costs of best scenarios rather than worst scenarios.

In addition, unit commitment scheduling highly depends on the risk level preferences, so when the operator changes the risk parameter, a new pattern of commitment will be obtained. In this simulation, choosing β close to one increases the participation of unit 3 which is an expensive and fast response back-up unit. This method shows that the risk-averse behavior of the operator would cope with severe incidents during operation day, and prepare more online units for mitigating disturbances. However, by increasing the value of β, the operator would have less concern for happening the worst scenarios, and unit 3 is online in fewer hours. In this case, the operator uses less power capacity of dispatchable units. Table 6 shows the commitment states of unit 3 in different risk management policies. In this table, one means online statues of DG3, and zero means that DG3 is not committed in some specific hours. Units 1 and 2 are the base generation units of microgrid, and have the same commitment statues in all strategies.

Table 6. Unit commitment states of DG3 in different risk strategies

beta	DG3 commitment hours (1–24)																							
	1	2	3	4	5	6	7	8	9	10	11	12	13	14	15	16	17	18	19	20	21	22	23	24
1	0	1	1	0	0	0	0	1	1	0	1	1	1	1	1	1	1	1	1	1	0	1	0	1
1.03	0	0	1	0	0	0	0	1	1	0	0	0	1	1	1	1	1	1	1	1	0	0	0	0
1.05	0	0	1	0	0	0	0	0	0	0	0	0	0	0	1	1	1	0	0	1	0	0	0	0

b) Confidence level (α)

Adjusting confidence level (α) enables the microgrid operator to classify expensive and cheap scenarios, so it has a pivotal role in managing the adverse consequences of expensive or worst scenarios.

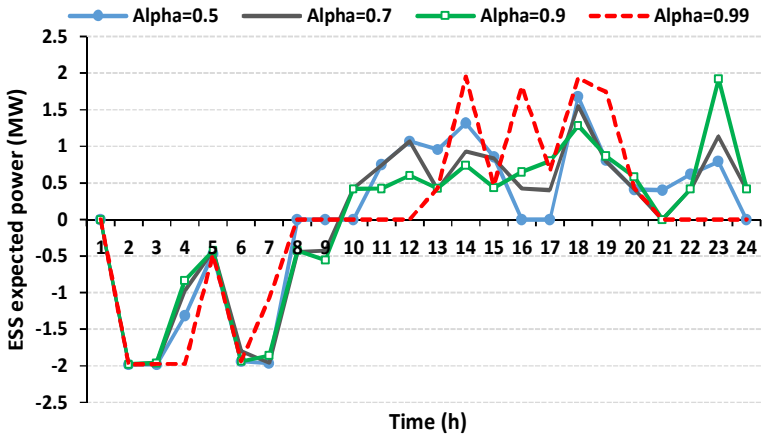

Fig. 13. ESS power charging/discharging patterns based on confidence level adjustment

For example, when α is adjusted at 0.7, it means that at least 30% of the expensive scenarios are constrained to the risk-averse policy, and almost 70% of other scenarios may be less considered by the operator in the scheduling process. Therefore, sensitivity analysis for α is crucial to discuss the influence of changing this parameter. By the way of illustration, Figure 13 clearly exhibits the effect of confidence level on ESS power charging and discharging. When α gets closer to the 1, ESS power is specifically scheduled to alleviate the adverse effect of scenario 5 which is the worst scenario. In this scenario, the islanding time period is between 13 pm

to 20 pm, and by α=0.99 the discharging hours happens exactly in islanded hours to beneficially use the resources for optimal operation. On the contrary, the fewer amount of α ensures different strategy in ESS scheduling, and it would provide a more smooth charging/discharging rate for ESS to virtually support all probable islanding hours based on different scenarios.

c) Piecewise linear approximation

The piecewise linear approximation method is used in non-linear formulations to maintain the problem statement linear. A linear representation of quadratic term like Equation (15a) is shown in Figure 14 using linear segments. The quadratic expression is formulated as (15b). Equation (15c) guarantees the predefined range of p in each linear segment. In these formulations, $i \in I$ shows the number of linear segments, and ψ_i^+ , ψ_i^- are defined as auxiliary variables. The obtained slope of linear segment is presented with α_i. Additional descriptions about the linearization procedure are represented in [15].

$$Z = p^2 \tag{15a}$$

$$Z = \sum_{i \in I} \alpha_i \times \psi_i^- + \sum_{i \in I} \alpha_i \times \psi_i^+ \tag{15b}$$

$$p = -\sum_{i \in I} \psi_i^- + \sum_{i \in I} \psi_i^+ \tag{15c}$$

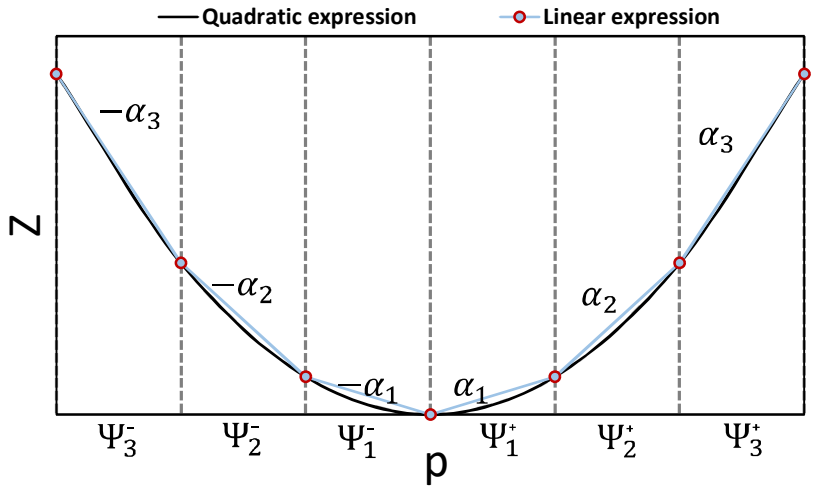

Fig. 14. The profiles of quadratic and linear functions

However, determining the appropriate number of pieces is so difficult. Few pieces may lead to imprecise results while choosing many pieces might increase the computation time of the problem. To circumvent this challenge, it is important to find sufficient pieces based on the technical issue. In Figure 15, the evolution of the microgrid operation cost versus the number of adopted pieces is depicted. It is evident that in the vicinity of 8 pieces, the expected cost stabilizes obviously. Hence, the accurateness of the numerical analysis is proved in this work.

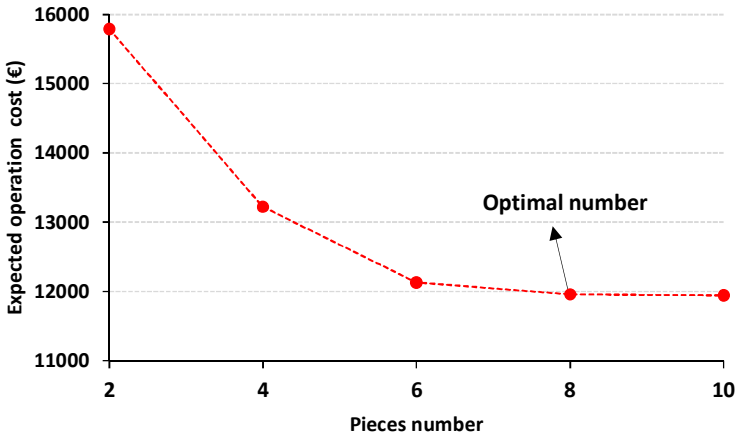

Fig. 15. Microgrid expected operation cost versus the number of selected pieces

6. Discussion

The proposed framework brings about advantages in operation of distribution systems as follows:

- The reactive market is included in the framework, which can be expected to be developed in future market designing as the penetration of Volt/VAR control devices and inverter-based generation units are increasing in distribution systems. Therefore, reactive power can be purchased from the owner of these units in the context of the reactive power market.
- Designing distribution market in power grid reduces fluctuation in transferred power between microgrid and distribution systems, ensuring the operational flexibility.
- The linearized model proposed in this study reduces the computation time of scheduling, making this model applicable in online operation.
- The equipment failure in main grid is modelled based on the MTTF and MTTR definitions to propose a realistic modeling of islanding based on the functionality and aging of the devices.
- Risk-averse scheduling strategy reduces the chance of experiencing high-cost scenarios, known as worst scenarios.

In this study, the role of the distribution market is just studied from microgrid's perspective. The two sides interaction of distribution market and microgrids can be studied in more comprehensive framework. Furthermore, the ISO can also be modeled in the operational model to determine the prices in market.

7. Conclusion

In this paper, a novel market-based scheduling was suggested, which considered the risk, distribution market operator (DMO) and linear approximation of AC power flow constraints in the mathematical framework. The proposed model was developed to give a comprehensive perspective on minimizing the day-ahead operation cost. The microgrid contained dispatchable units, ESS, wind turbines and DR resources. The uncertainties of the active and reactive loads, wind power and main grid equipment failure were simulated, and a realistic microgrid islanding model was proposed. The model used the capacity of available resources for economic operation and demonstrated the interaction with DMO. A typical test system was implemented to investigate the capability of the market-based model under different evaluations. The numerical results showed that having interaction with DMO reduced the negative impacts of uncertainties, and improved the reliability and efficiency of microgrid operation as it could reduce peak loads of the system. It was observed that in some hours the operator could prefer to deviate from DMO's power profile to compensate the energy shortages or to provide more economic operation. Furthermore, it was shown that, based on optimal scheduling, most ESS discharging power capacity (i.e., 76%) was devoted to islanded hours to diminish the load shedding. The effect of the risk-averse strategy was discussed on reducing the operation cost of worst scenarios, and the sensitivity of the cost of each scenario to the β adjustment was explained in detail. Moreover, dispatchable units' generation increased when the operator concerned about the risk of high-cost scenario since units were kept online to hedge against the probable expensive incident. Moreover, increasing the confidence level intensified the variation of the ESS charging/discharging pattern, and the highest confidence level led to mitigate the unfavorable effect of fewer and expensive scenarios. Finally, in order to demonstrate the accuracy of the proposed model, the piecewise linear approach and finding the best number of pieces was examined.

As for the future work, we will try to develop a comprehensive model in which the microgrid has the chance to change the assigned power and price signals in a competitive market-based environment. Moreover, the role of reactive market will be investigated more considering inverter-based technologies and solar generation units in microgrid. Also, the microgrid will be able to sell the reactive power to the distribution market based on the reactive power generated by inverter-based resources during the operation time.

8. References

[1] Z. Li, and Y. Xu, "Optimal coordinated energy dispatch of a multi-energy microgrid in grid-connected and islanded modes," *Applied Energy,* vol. 210, pp. 974-986, 2018.

[2] M. Hemmati, B. Mohammadi-ivatloo, M. Abapour, and A. Anvari-Moghaddam, "Optimal Chance-Constrained Scheduling of Reconfigurable Microgrids Considering Islanding Operation Constraints," *IEEE Systems Journal,* pp. 1–10, 2020, DOI: 10.1109/JSYST.2020.2964637

[3] A. A. Bashir, M. Pourakbari-Kasmaei, J. Contreras, and M. Lehtonen, "A novel energy scheduling framework for reliable and economic operation of islanded and grid-connected microgrids," *Electric Power Systems Research,* vol. 171, pp. 85-96, 2019.

[4] S. M. Hashemi, V. Vahidinasab, M. S. Ghazizadeh, and J. Aghaei, "Valuing consumer participation in security enhancement of microgrids," *IET Generation, Transmission & Distribution*, vol. 13, no. 5, pp. 595-602, 2019.

[5] M. V. Castro, C. Moreira, and L. M. Carvalho, "Hierarchical optimisation strategy for energy scheduling and volt/var control in autonomous clusters of microgrids," *IET Renewable Power Generation*, vol. 14, no. 1, pp. 27–38, 2020.

[6] J. Zhu, T. Zhu, X. Mo, and M. Liu, "A spatiotemporal decomposition algorithm for fully decentralized dynamic economic dispatch in a microgrid," *Electric Power Systems Research,* vol. 189, 106564, 2020.

[7] A. Shokri Gazafroudi, J. Manuel Corchado, A. Keane, and A. Soroudi," Decentralised flexibility management for EVs," *IET Renewable Power Generation*, vol. 13, no. 6, pp. 952–960, 2019.

[8] M. Mehdi, C. H. Kim, and M. Saad, "Robust Centralized Control for DC Islanded Microgrid Considering Communication Network Delay," *IEEE Transactions on Industry Applications*, vol. 9, pp. 77765–77778, 2020.

[9] A. Rezaee Jordehi, M. S. Javadi, M. Shafie-khah, and J. P. S. Catalão, " Information gap decision theory (IGDT)-based robust scheduling of combined cooling, heat and power energy hubs," *Energy,* vol. 231, 120918, 2021.

[10] H. Geramifar, M. Shahabi, and T. Barforoshi, "Coordination of energy storage systems and DR resources for optimal scheduling of microgrids under uncertainties," *IET Renewable Power Generation,* vol. 11, no. 2, pp. 378-388, 2017.

[11] M. H. Shams, M. Shahabi, M. MansourLakouraj, M. Shafie-khah, and J. P. S. Catalão, " Adjustable robust optimization approach for two-stage operation of energy hub-based microgrids," *Energy,* vol. 222, 119894, 2021.

[12] C. Zhang, Y. Xu, Z. Li, and Z.Y. Dong, "Robustly Coordinated Operation of a Multi-Energy Microgrid with Flexible Electric and Thermal Loads," *IEEE Transactions on Smart Grid,* vol. 10, no. 3, pp. 2765-2775, 2019.

[13] M. H. Shams, M. Shahabi, and M. E. Khodayar, "Stochastic day-ahead scheduling of multiple energy carrier microgrids with demand response," *Energy,* vol. 155, pp. 326-338, 2018.

[14] S. Bahramirah, A. Khodaei, and R. Masiello, "Distribution Markets," *IEEE Power and Energy Magazine*, vol. 14, no. 2, pp. 102 – 106, 2016.

[15] M. Mansour-lakouraj, and M. Shahabi, "Comprehensive analysis of risk-based energy management for dependent micro-grid under normal and emergency operations," *Energy,* vol. 171, pp. 928-943, 2019.

[16] S. Parhizi and A. Khodaei, "Market-based microgrid optimal scheduling," *IEEE International Conference on Smart Grid Communication. (SmartGridComm)*, Miami, FL, USA, pp. 55–60, 2015.

[17] S. Parhizi, A. Khodaei, and M. Shahidepour, "Market-Based Versus Price-Based Microgrid Optimal Scheduling," *IEEE Transactions on Smart Grid*, vol. 9, no. 2, pp. 615 – 623, 2018.

[18] M. MansourLakouraj, M. Shahabi, M. Shafie-khah, N. Ghoreishi, and J. P. S. Catalão, " Optimal power management of dependent microgrid considering distribution market and unused power capacity," *Energy,* vol. 200, 117551, 2020.

[19] A. Alanazi, H. Lotfi, and A. Khodaei, "Market clearing in microgrid-integrated active distribution networks," *Electric Power Systems Research,* vol. 183, 106263, 2020.

[20] A. J. Conejo, M. Carrión, and J. M. Morales, "Decision making under uncertainty in electricity markets," Springer, 2010.

[21] M. MansourLakouraj, M. S. Javadi, and J. P. Catalão., "Flexibility-Oriented Scheduling of Microgrids Considering the Risk of Uncertainties," *International Conference on Smart Energy Systems and Technologies (SEST)*, 2020.

[22] GAMS/SCENRED Documentation. [Online]. Available: www.gams.com/docs/document.htm.

[23] L. Bai, J. Wang, C. Wang, C. Chen, and F. Li, "Distribution Locational Marginal Pricing (DLMP) for Congestion Management and Voltage Support," *IEEE Transactions on Power Systems*, vol. 33, no. 4, pp. 4061-4073, 2017.

[24] A. Safdarian, M. Fotuhi-Firuzabad and F. Aminifar, "A new formulation for power system reliability assessment with AC constraints," *Electrical Power and Energy Systems,* vol. 56, pp. 298-306, 2014.

[25] M. MansourLakouraj, M. S. Sanjari, M. S. Javadi, M. Shahabi, and J. P. Catalão " Exploitation of Microgrid Flexibility in Distribution System Hosting Prosumers, " *IEEE Transactions on Industry Applications,* vol. 57, pp. 4222-4231, 2021.

[26] M. Mazidi, A. Zakariazadeh, S. Jadid, and P. Siano, "Integrated scheduling of renewable generation and demand response programs in a microgrid," *Energy Conversion and Management,* vol. 86, pp. 1118-1127, 2014.

[27] S. M. B. Sadati, J. Moshtagh, M. Shafie-khah, A. Rastgou, and J. P. S. Catalão, "Bi-level model for operational scheduling of a distribution company that supplies electric vehicle parking lots," *Electric Power Systems Research,* vol. 174, 2019.

[28] A. Safdarian, M. Fotuhi-Firuzabad and M. Lehtonen, "A Stochastic Framework for Short-Term Operation of a Distribution Company ," *IEEE Transactions on Power Systems,* vol. 28, pp. 4712-4721, 2013.

[29] "NREL: Western Wind Resources Dataset, " [Online]: http://wind.nrel.gov/web_nrel

[30] M. BiazarGhadikolaei, M. Shahabi, and T. Barforoshi, "Expansion planning of energy storages in microgrid under uncertainties and demand response," *Int Trans on Electr Energ Syst.*, 2019; e1210.https://doi.org/10.1002/2050-7038.1210